Available online at www.sciencedirect.com
ScienceDirect
Journal of Crystal Growth 301–302 (2007) 324–329
JOURNAL OF CRYSTAL GROWTH
www.elsevier.com/locate/jcrysgro

Isotopically controlled self-assembled Ge/Si nanostructures

O. Moutanabbir*, S. Miyamoto, A. Fujimoto, K.M. Itoh

Department of Applied Physics and Physico-Informatics, Keio University, 3-14-1 Hiyoshi, Kohoko-ku, Yokohama 223-8522, Japan

Available online 26 January 2007

Abstract

By combining Raman scattering and stable Ge isotopes tracing, we present a new analytical procedure to address the stability of 2D Stranski–Krastanov WL during 3D transition. Our approach is based on the experimentally verified fact that WL has no clear Raman modes and on the dependency of phonon frequencies on the isotopic composition. A direct quantification of the amount of material transferred from WL to 3D islands was achieved for Ge epitaxy on HF-etched Si(0 0 1). The estimated isotopic abundance suggests an exchange process between WL atoms and Ge atoms from direct flux during the growth of island. The influence of surface preparation on islands morphology is also investigated. We found that the growth on HF-etched Si(0 0 1) induces a low density of large dome-like islands. Carbon contaminants seem to play a critical role in self-assembling of Ge islands on hydrophobic Si(0 0 1) surface.

PACS: 68.55.Ac; 68.65.Hb; 81.15.Hi; 68.47.Fg; 78.30.−j

Keywords: A1. Nanostructures; A3. Molecular beam epitaxy; B1. Germanium silicon alloys

1. Introduction

A wide variety of quantum heterostructures has become possible because of dramatic improvements in semiconductor materials that can be successfully grown from III–V, II–VI, and Group-IV lattice-mismatched semiconductors [1]. Among the different material combinations investigated, the Ge/Si heteroepitaxial system was the subject of numerous studies in the last decade, both from a fundamental point of view and for potential applications [2]. Deposition of Ge on Si is a model of Stranski–Krastanov system which is characterized by a transition from an initial layer-by-layer regime to 3D islanding [3]. The transition is driven by the elastic strain, which becomes too large to form a dislocation-free flat layer and is partially released by the formation of 3D clusters. The phenomenon is further complicated by alloying, i.e., Si–Ge interdiffusion, which provides another pathway for the elastic strain relaxation. From a technological point of view, the Ge/Si 3D islands are good candidates to fabricate QDs, i.e., structures in which the charge carriers are confined in atomic-like potentials. The controlled growth of such QDs could represent a real breakthrough in the optoelectronics sector, allowing to integrate microelectronic and optoelectronic circuits on the same Si wafer.

However, it is still a challenge to obtain QDs with a high uniformity both in size and spatial distribution in order to exploit their unique properties in novel devices. In this context, several approaches were explored aiming at controlling the placement and arrangements of Ge dots by introducing periodic morphological features on the surface or by manipulating its chemistry by predeposition of impurities [4]. In addition to QDs engineering challenges, considerable work has been devoted for understanding and modelling of the microscopic mechanisms of the epitaxial island growth. Vastly different results in literature unavoidably open up the discussion about the very fundamental processes occurring during the growth. The interesting physics question is by what precise atomic mechanisms Ge/Si islands nucleate and grow. There is no universal answer.

Although Ge/Si self-assembled islands are grown on top of the WL, some theoretical and experimental studies omit

*Corresponding author. Present address: Max-Planck-Institut für Mikrostrukturphysik, Weinberg 2D - 06120 Halle, Germany.
Fax: +49 345 551 1223.
E-mail address: moutanab@mpi-halle.mpg.de (O. Moutanabbir).

0022-0248/$ - see front matter © 2006 Elsevier B.V. All rights reserved.
doi:10.1016/j.jcrysgro.2006.11.178

the WL from their simulations or investigations without much justification. Others including the WL only briefly discuss its influence on the properties of 3D islands. However, mass transport on the surface of WL underlies most of the other detailed mechanisms of islands nucleation and growth. Hence, a quantitative determination of WL–3D interdiffusion is of particular significance, both for improving our understanding of the microscopic mechanisms of self-organization, and also as a primary input for epitaxial growth models and calculations.

In this work, we report a new approach for investigating subtle points in surface mass transport during growth of Ge/Si nanostructures. We propose an isotope variation of Stranski–Krastanov growth process in which the isotopic composition of 2D WL and the impinging Ge atoms flux during 3D growth is rigorously controlled. In addition to their technological promise in quantum computing, nanoscience, and spintronics, the scientific interest and increased availability of highly enriched isotopes have led to a sharp rise in the number of experimental and theoretical studies of isotopically controlled semiconductor crystals [5]. The absence of any chemical, mechanical, or electrical driving forces makes possible the study of an ideal random-walk problem, in which moving atoms go in random directions at random intervals. The most conspicuous effects observed have to do with the dependence of phonon frequencies on isotopic composition. Based on this peculiarity, Raman scattering spectroscopy (RSS) was used to determine both the isotopic composition of the grown nanostructures and its evolution during Ge evaporation. In this work, we applied this approach to investigate Ge epitaxy on HF-etched Si(0 0 1) surfaces. Using hydrophobic surfaces, we found that island morphology shows a dramatic change compared to the growth on surfaces cleaned using the conventional hydrophilic procedure. These observations are discussed in terms of carbon contaminants influence.

2. Methodology

Our molecular beam epitaxy (MBE) system is equipped with several pure Ge isotopes sources. In the proposed approach, we used ^{70}Ge and ^{76}Ge sources to grow Ge/Si islands in a two-step process. First, a planar WL is grown by deposition of pure ^{76}Ge. In the second step, 2D–3D transition is immediately achieved by an additional evaporation of pure ^{70}Ge. As a reference, single isotope islands (i.e., both WL and 3D structures were obtained using the same isotope ^{70}Ge/^{70}Ge/Si) were grown in order to eliminate the influence of in-plane strain on phonon frequencies in our analytical procedure. The growth of these two-isotope heterostructures is schematically illustrated in Fig. 1. Based on this growth process, the interaction between WL atoms and evaporated atoms during growth of 3D nanostructures can be investigated. Since phonon frequencies depend on isotopic composition, ^{76}Ge "impurities" are used as a marker to evidence and quantitatively analyze the mass transport from 2D WL to 3D Ge/Si islands.

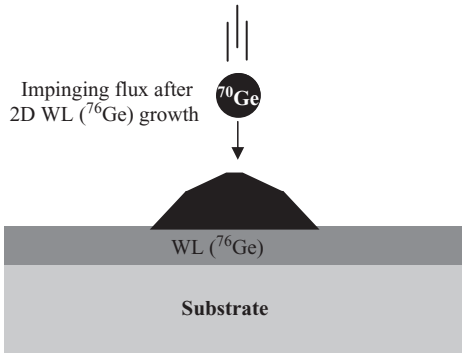

Fig. 1. Schematic cross section of isotopically controlled Ge/Si heteroepitaxy in an abrupt interfaces configuration. Two pure isotopes are used: ^{76}Ge for the growth of planar WL, and ^{70}Ge for the growth of 3D islands.

It is well established that the Ge WL does not contribute to Raman signal [6,7], i.e., the detected modes are attributed to 3D islands. In an abrupt epitaxy, phonon modes frequencies must be the same for both single isotope ^{70}Ge/^{70}Ge/Si and two-isotope ^{70}Ge/^{76}Ge/Si islands since in both configurations the grown islands would be formed by pure ^{70}Ge. However, in a more realistic picture, ^{76}Ge atoms (i.e., WL atoms) diffusion into 3D structures will induce a shift in their Ge–Ge and Si–Ge mode frequencies. In this case, the virtual-crystal approximation is valid and results in a proportionality of any phonon frequencies on the inverse of the square root of the mass [5]. The effects of the average isotopic mass just mentioned are the simplest isotopic effects possible since they appear in the harmonic approximation.

By introducing the isotopic composition, the stoichiometry of our nanostructures will be $(^{70}Ge_{1-y}{}^{76}Ge_y)_xSi_{1-x}$, where x is Ge concentration in the islands and y is the isotopic abundance of ^{76}Ge. y presents also the amount of Ge WL material transferred to 3D islands which can be estimated from

$$y = \left[\frac{1}{m(^{76}\mathrm{Ge})/m(^{70}\mathrm{Ge}) - 1}\right] \times \left[\frac{1}{[1 - \delta w/w_{^{70}\mathrm{Ge}}]^2} - 1\right], \quad (1)$$

where $w_{^{70}\mathrm{Ge}}$ is Ge–Ge mode frequency measured for single isotope islands (^{70}Ge/^{70}Ge/Si), δw is the shift induced by ^{76}Ge atoms diffusion defined as $w_{^{70}\mathrm{Ge}} - w_{^{70}\mathrm{Ge}/^{76}\mathrm{Ge}}$, where $w_{^{70}\mathrm{Ge}/^{76}\mathrm{Ge}}$ is Ge–Ge mode frequency measured for two-isotope islands (^{70}Ge/^{76}Ge/Si). Finally, $m(^{70}\mathrm{Ge})$ and $m(^{76}\mathrm{Ge})$ represent atomic masses of ^{70}Ge and ^{76}Ge isotopes, respectively.

In order to reduce the experimental error, several reference samples with well controlled isotopic abundance were grown using pure beams ^{76}Ge ($y = 1$) and isotopically mixed beam $^{70}Ge_{0.5}{}^{76}Ge_{0.5}$ ($y = 0.5$). In this case, the contribution of WL atoms to island formation can be obtained graphically using the linear function $y = f(w_{\mathrm{Ge}}^{-2})$.

3. Experimental details

Preparation of the wafer surface is a critical step in any epitaxy recipe. For Si wafers, two approaches have been taken. In the first, a chemical oxide is formed *ex situ* and then thermally desorbed *in situ*. This surface preparation procedure is commonly known as Ishizaka–Shiraki method which is widely used in Ge/Si heteroepitaxy [8]. However, it is not always suitable due to high temperature needed which cannot be compatible with some newly developed QDs engineering processes [9]. In the second, the native oxide is removed with an acid treatment and the resulting hydrides are thermally desorbed *in situ*, at temperatures hundreds of degrees lower than those needed to desorb the oxide [10,11]. In this work, a set of 2 in Si(0 0 1) wafers were chemically cleaned by H_2SO_4:H_2O_2 (2:1) solution and the surface was H-terminated by a dip in aqueous 2.5% HF. It is worth noting that after the final etching step, the samples were briefly rinsed in deionized water in order to remove minority species. Subsequently, the substrates were loaded into MBE chamber and heated at 540 °C for 1 h. The growth was monitored *in situ* by reflection high-energy electron diffraction (RHEED), and the island topography was studied *ex situ* by atomic force microscopy (AFM). AFM images were statistically analyzed using WS×M program [12]. RSS spectra were recorded in backscattering geometry using Jobin Yvon/Horiba T64000 micro-Raman system equipped with an Olympus microscope. Measurements were performed at room temperature with 514.5 nm line from an argon ion laser. A spot diameter of about 3 μm was used throughout the study and the power density was kept very low to prevent sample heating. The position, intensity, and width of Raman lines due to local Ge–Ge, Ge–Si, and Si–Si modes of the Ge/Si alloy enable one to obtain information on the composition, strain, and confinement within the Ge–Si nanostructures [13].

4. Results and discussion

In AFM images (not shown), quite a surprising behavior can be pointed out: islands size, shape and density are profoundly affected by substrate surface preparation procedure. In fact, we note that on the wafer cleaned by the conventional hydrophilic procedure a high density of the so-called hut clusters with an elongated pyramidal shape formed by {1 0 5} facets. Whereas, the deposition of the same amount of Ge on HF-etched Si surface, after a complete desorption of hydrogen, results on a lower density of larger Ge/Si islands with a dome-like morphology with no clear faceting (height ~25 nm and diameter ~130 nm).

The origin of this dependency of islands morphology on substrate cleaning can be found in RHEED patterns of HF-etched Si(0 0 1) surface recorded at different temperatures [14]. We found that around the growth temperature, the surface exhibits a (2 × 1) pattern characteristic of a clean surface after the complete hydrogen desorption. However, the pattern is very diffuse compared to the one obtained using the conventional Ishizaka–Shiraki cleaning procedure. This indicates that HF-etched surfaces are very rough and disordered. Interestingly, by increasing the substrate temperature the pattern changed into a c(4 × 4) structure. Moreover, we found that the c(4 × 4) reconstruction is only observable in a narrow window of temperature. In fact, after a further increasing of temperature, the c(4 × 4) pattern gradually disappeared and was replaced by a SiC transmission pattern. This thermal evolution from the surface reconstruction to the bulk diffraction pattern indicates that the c(4 × 4) reconstruction is related to carbon [10]. Consequently, the observed morphological change on Ge/Si islands can be understood as an influence of carbon contaminants. In fact, several works have demonstrated that common laboratory air can be a source of carbon (or carbon bearing) impurities on H-passivated silicon surfaces [15]. The influence of carbon on Ge/Si heteroepitaxy was the subject of numerous studies in which carbon impurities were intentionally introduced [16]. The pre-deposition of a fraction of a monolayer of C on Si(0 0 1) creates an inhomogeneous $Si_{1-x}C_x$ layer that strongly influences island formation. Direct observation of carbon-induced c(4 × 4) reconstruction on Si(0 0 1) surface hints at a selective deposition of Ge in carbon-free regions. The repulsive interaction between Ge and C may also contribute to this selective growth [16].

In order to investigate the surface mass transport during Ge/Si islands growth on HF-etched Si, we used the approach described in Section 3. The exact critical thickness of 2D–3D transition was estimated by using *ex situ* AFM analysis and found to be 2.5 ML. We note that 3D transition on HF-etched Si(0 0 1) surfaces occurs earlier compared to the conventional cleaned surfaces where islanding starts at ~4 ML. Raman spectra were recoded for Ge coverage ranging from 4 ML (1.5 ML + WL) to 9 ML (6.5 ML + WL). At each coverage, in addition to two-istope islands $^{70}Ge/^{76}Ge/Si$, three standard samples were grown: $^{70}Ge/Si$, $^{76}Ge/Si$, and $^{70}Ge_{0.5}{}^{76}Ge_{0.5}/Si$. AFM analysis shows the same morphology for different configurations at a given Ge coverage. It is worth noting that in the case of atomically mixed beams $^{70}Ge_{0.5}{}^{76}Ge_{0.5}$, the growth rate of each source was adjusted to obtain a total growth rate similar to that of single isotope epitaxy.

Fig. 2 displays a representative set of Raman spectra recorded for a total Ge coverage of 5 ML (2.5 ML + WL). For comparison, Si(0 0 1) substrate Raman spectrum (dots) is also shown. WL Raman spectrum (not shown) was found to be similar to Si(001) substrate signal indicating that no clear Raman modes are related to WL in agreement with previous studies [6,7]. It is obvious that some spectral features in the Raman spectrum of Ge/Si samples are related to the Si layers, such as the peaks at ~301 and 435 cm^{-1} which originate from the two-phonon scattering of 2TA(X) and 2TA(Σ), respectively. The intrinsic Raman spectra of Ge/Si islands are obtained by subtracting the spectrum of pure Si substrate from the measured spectra.

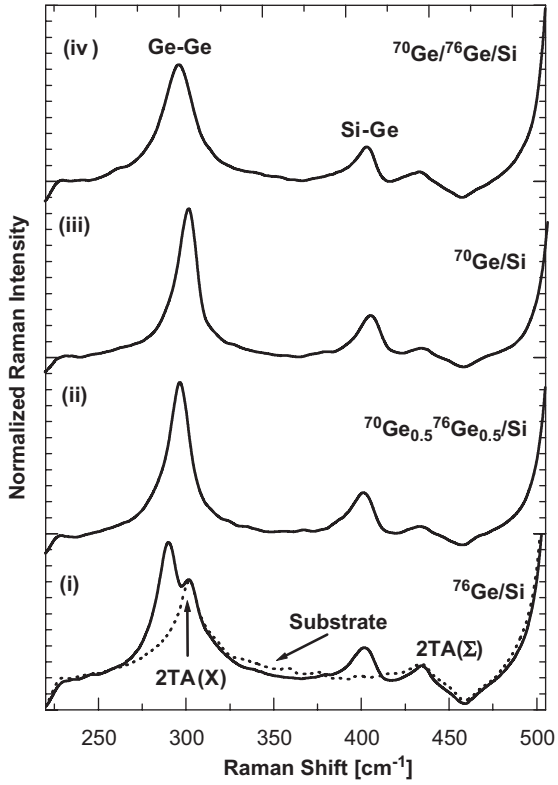

Fig. 2. Raman spectra of Ge/Si(0 0 1) nanostructures grown by deposition of 5 ML of Ge at 540 °C: (i) ^{76}Ge; (ii) ^{70}Ge$_{0.5}$^{76}Ge$_{0.5}$; (iii) ^{70}Ge; and (iv) ^{70}Ge/^{76}Ge. As a reference, Si(0 0 1) substrate Raman spectrum (dots) is also shown.

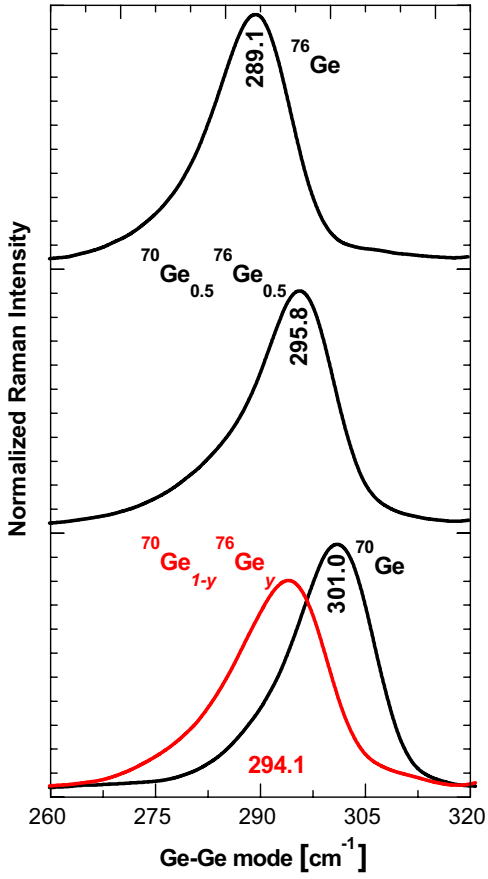

Fig. 3. Ge–Ge mode of the grown isotopically controlled Ge/Si nanostructure: two-istope sample ^{70}Ge/^{76}Ge (red line) and reference samples (black lines).

Using empirical relations [6,7], the intensities of Ge–Ge and Si–Ge modes were used to estimate the average Ge content x in islands. We found that Ge composition slightly decreases from 0.85 at the lowest coverage to 0.75 at the highest coverage corresponding to an average Si content of 0.15 and 0.25, respectively. In the other hand, the total volume of islands grown at coverage ranging from 4 to 9 ML corresponds to the volume of a film of circa ranging from 5.85 to 13.4 ML as determined by AFM. This extra volume (an increase of ~45–50%) cannot be explained by a simple Si–Ge alloying. Ge WL atom migration towards islands seems to play an important role in the observed increasing of islands volume. Such mass diffusion from WL to 3D structures during the early stage of nucleation has been suggested by *in vivo* STM studies indicating a strong diffusion of material from 2D WL to 3D islands [17].

A direct evidence of the contribution of WL atoms to the formation of the islands can be found in Fig. 3. In this figure, we show Ge/Si islands intrinsic Raman spectra in Ge–Ge LO phonon region for two-isotope structures in comparison with reference samples grown at 5 ML. We note that in two-isotope islands the Ge–Ge mode is shifted down by ~6 cm^{-1} from its frequency in pure ^{70}Ge islands. As it is mentioned above, in the case of an abrupt epitaxy in these configurations Ge–Ge mode would have the same frequency. Thus, the observed shift is simply induced by ^{76}Ge atoms diffusion from WL to 3D islands. We note also that Ge–Ge peak is broader in the case of two-isotope islands indicating that atoms from WL and those from direct flux are not homogeneously distributed inside Ge/Si structures.

By using the proportionality between the average isotopic mass and w_{Ge}^{-2}, the fraction of atoms initially from WL forming 3D structures can be estimated (Fig. 4). We note that at 5 ML about 58% of Ge atoms in islands are coming from WL. This suggests that atoms from direct flux evaporated during 3D growth represent ~ 42% of island Ge composition. The contribution of WL atoms to 3D islands is slightly higher at 4 ML, but it decreases dramatically at 6 ML and stays almost constant up to 9 ML, as shown in Fig. 5 displaying the evolution WL atoms induced shift of Ge–Ge mode (δw_{GeGe}) and their content in 3D structures (y) as a function of Ge coverage. We note that the evolution of y with the evaporated amount of Ge presents two different regimes at low and high coverage. At low coverage regime (4–5 ML), WL atoms present roughly 60% of all Ge atoms forming the grown heterostructures. Obviously, Ge atoms migration from WL towards 3D islands cannot explain alone the observed isotopic composition. In fact, for instance in the

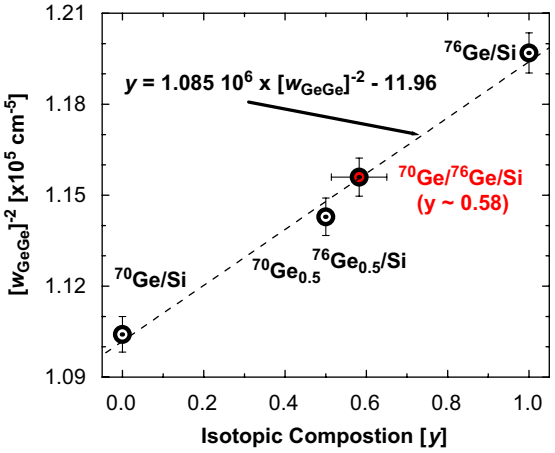

Fig. 4. Estimation of isotopic abundance of ^{76}Ge in ^{70}Ge/^{76}Ge nanostructures (red dot). The linear fit is obtained within the harmonic approximation.

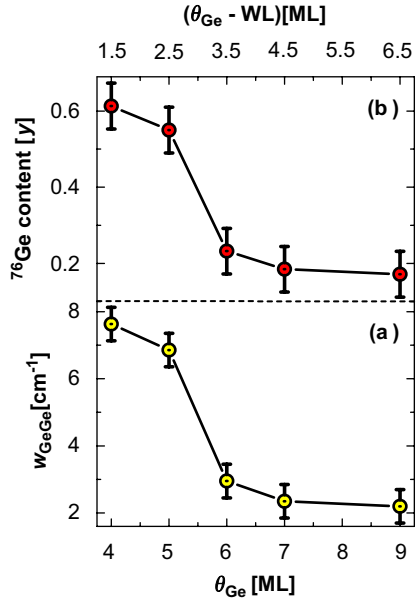

Fig. 5. Evolution as a function of Ge coverage of: (a) Ge–Ge mode shift induced by WL atoms diffusion into 3D islands; and (b) the contribution of Ge WL atoms to the formation of the islands.

case of 5 ML, even if all WL material is transformed into 3D islands the observed isotopic composition (y~0.6) can never be reached. An exchange process between Ge atoms from WL and those coming form direct flux during 3D growth may be a plausible scenario for these observations. Additionally, we note that at the high Ge coverage regime ($>$ 5 ML), the isotopic abundance of ^{76}Ge decreases dramatically compared to low coverage regime.

A possible contribution of carbon contaminants to the observed evolution cannot be evidenced from these measurements. An additional set of measurements on Ge islands grown on carbon-free Si(0 0 1) is required to verify the influence of carbon contaminants on surface mass transport process and WL–3D interactions during the growth of Ge islands. From the previous studies [16], one may expect that the presence of carbon at the surface may affect the diffusivity process describing the random walk of the surface event that dominates the mass transport. The observed decrease in island density suggests that carbon can arrange in metastable surface sites which are responsible for the increase of adatom mobility. Alternatively, the reduction of islands density can also be explained by a reduction of the available sites for the growth on the surface due to HF etching induced roughening and microscopic faceting.

5. Conclusion

In summary, we proposed a new approach to highlight subtle points in the growth of self-assembled Ge/Si heterostructures. By combining Raman scattering and stable Ge isotopes tracing, we presented an analytical tool to address the stability of 2D Stranski–Krastanov WL during 3D transition. Our approach is based on the experimentally verified fact that WL has no clear Raman modes and on the dependency of phonon frequencies on the isotopic composition. A direct quantification of the amount of material transformed from WL to 3D islands was achieved for Ge epitaxy on HF-etched Si(0 0 1). The estimated isotopic abundance suggests an exchange process between WL atoms and Ge atoms from direct flux during the growth of island. Using hydrophobic surfaces, we found that island morphology shows a dramatic change compared to the growth on surfaces cleaned using the conventional hydrophilic procedure. Carbon contaminants trapping on H-passivated Si(0 0 1) surfaces seem to play a key role on the observed morphology.

References

[1] D. Bimberg, M. Grundmann, N.N. Ledentsov, Quantum Dot Heterostructures, Wiley, Chichester, 1999.
[2] J. Stangl, V. Holy, G. Bauer, Rev. Mod. Phys. 76 (2004) 725.
[3] I.N. Stranski, L. Krastanov, Zur Theorie der orientierten Ausscheidung von Ionenkristallen aufeinander, Sitzungsber. Akad. Wiss. Wien, Math. Naturwiss. Kl. llb 146 (1938) 797.
[4] J.-M. Baribeau, X. Wu, N.L. Rowell, D.J. Lockwood, J. Phys. Condens. Matter 18 (2006) R139.
[5] M. Cardona, M.L.W. Thewalt, Rev. Mod. Phys. 77 (2005) 1173.
[6] P.H. Tan, K. Brunner, D. Bougeard, G. Abstreiter, Phys. Rev. B 68 (2003) 125302.
[7] A.V. Baranov, A.V. Federov, T.S. Perova, R.A. Moore, V. Yam, D. Bouchier, V. Lethanh, K. Berwick, Phys. Rev. B 73 (2006) 075322.
[8] A. Ishizaka, Y. Shiraki, J. Electrochem. Soc. 133 (1986) 666.
[9] J.T. Robinson, J.A. Liddle, A. Minor, V. Radmilovic, D.O. Yi, P. Alex Greany, K.N. Long, D.C. Chrzan, O.D. Dubon, Nano Lett. 5 (2005) 2070.
[10] K. Miki, K. Sakamoto, T. Sakamoto, Surf. Sci. 406 (1998) 312.
[11] V. Le Thanh, D. Bouchier, D. Debarre, Phys. Rev. B 56 (1997) 10505.

[12] WSxM program, Nanotech Electronica, C/Padilla 1, 28006 Madrid, Spain, ⟨http://www.nanotec.es⟩.
[13] K. Brunner, Prog. Theor. Phys. 65 (2002) 27.
[14] O. Moutanabbir, S. Miyamoto, K.M. Itoh, unpublished.
[15] See for e.g., S. Kasi, M. Liehr, P. Thiry, H. Dallaporta, M. Offenberg, Appl. Phys. Lett. 59 (1990) 108.
[16] O. Leifeld, A. Beyer, D. Grutzmacher, K. Kern, Phys. Rev. B 66 (2002) 125312;
P.C. Kelires, Phys. Rev. Lett. 75 (1995) 1114;
A. Bernardi, J.O. Osso, M.I. Alonso, A.R. Goni, M. Garriga, Nanotechnology 17 (2006) 2602.
[17] B. Voigtländer, Surf. Sci. Rep. 43 (2001) 127.